Journal of Palaeogeography, 2016, 5(3): 185–204 (00096)

Available online at www.sciencedirect.com

ScienceDirect

journal homepage: http://www.journals.elsevier.com/journal-of-palaeogeography/

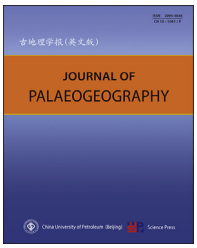

Lithofacies palaeogeography and sedimentology

Research on the architecture of submarine-fan lobes in the Niger Delta Basin, offshore West Africa

Jia-Jia Zhang [a], *Sheng-He Wu* [a,*], *Ting-En Fan* [b], *Hong-Jun Fan* [b], *Li Jiang* [a], *Cheng Chen* [a], *Qiong-Yuan Wu* [a], *Peng Lin* [a]

[a] *State Key Laboratory of Petroleum Resources and Prospecting, College of Geosciences, China University of Petroleum (Beijing), Beijing 102249, China*

[b] *Research Institute, China National Offshore Oil Corporation, Beijing 100010, China*

Abstract As one of the most important reservoirs in submarine fan, submarine lobes are hot fields for the deep-water oil–gas exploration in the world. Although a large amount of researches have been carried out on the architecture model of submarine lobes throughout the world, some controversies still exist on aspects such as the differential distribution of composite patterns and the quantitative relationships among different sedimentary settings. This paper, which took an oilfield in the Niger Delta Basin offshore West Africa as an example and utilized abundant core, well-logging and seismic data comprehensively, established the semi-quantitative to quantitative architecture model for individual lobe and lobe complex.

Results show that (1) A lobe complex was composed of multiple individual lobes as the compensational stacking pattern. According to the stacked relationship among individual lobes, four types of compensational stacking pattern were classified as the inordered type, the lateral migration type, the retrograding type and the prograding type. Influenced by the laterally confined degree of palaeotopography, the basin floor fan lobe complex was easily superimposed as inordered type, showing relatively large lateral width but relatively small thickness; the slope fan lobe complex was easily superimposed as lateral migration, retrograding and prograding types, showing relatively small lateral width but relatively large thickness. (2) Influenced by the laterally confined degree of palaeotopography, the basin floor fan individual lobes showed relatively large planar distribution area but relatively small thickness, while the slope fan individual lobes showed relatively small planar distribution area but relatively large thickness. An individual lobe was composed of multiple lobe stories by the way of aggradation–progradation pattern. From proximal to middle and distal part of individual lobes, the bottom mass-transport-deposits and the top branch channels disappeared gradually, and the amalgamated degree of the middle tabular sandbodies weakened as well with gradually developing of muddy interlayers. The formation of an individual lobe generally includes three stages as "rapid accumulation–progradation–aggradation".

Keywords Submarine lobes, Composite pattern, Quantitative scale, Niger Delta Basin, West Africa

* Corresponding author.
E-mail address: reser@cup.edu.cn (S.-H. Wu).
Peer review under responsibility of China University of Petroleum (Beijing).
http://dx.doi.org/10.1016/j.jop.2016.05.005
2095-3836/© 2016 China University of Petroleum (Beijing). Production and hosting by Elsevier B.V. on behalf of China University of Petroleum (Beijing). This is an open access article under the CC BY-NC-ND license (http://creativecommons.org/licenses/by-nc-nd/4.0/).

© 2016 China University of Petroleum (Beijing). Production and hosting by Elsevier B.V. on behalf of China University of Petroleum (Beijing). This is an open access article under the CC BY-NC-ND license (http://creativecommons.org/licenses/by-nc-nd/4.0/).

Received 3 December 2015; revised 4 January 2016; accepted 7 January 2016; available online 10 May 2016

1. Introduction

Submarine lobes, which are lobate sedimentary bodies developed at the end of submarine channels, are one of most important reservoirs in submarine fan (Beaubouef *et al.*, 2003; Chapin *et al.*, 1994; Posamentier and Kolla, 2003; Reading and Richards, 1994; Shanmugam and Moiola, 1991; Walker, 1978; Weimer and Slatt, 2006). Submarine lobes exhibit much complicated architecture hierarchy, which generally involves lobe complex, individual lobe, lobe story and smaller architecture unites, although a uniform scheme remains to be established as a result of the much varied scale of research objectives (outcrops, modern seafloor sedimentation, substrate reservoirs) by different authors (Deptuck *et al.*, 2008; Mutti and Normark, 1987; Prélat *et al.*, 2009, 2010). Mutti and Sonnino (1981) first proposed that a lobe complex was composed of multiple individual lobes in the way of compensational stack, a priority of lobes depositing at topographic lows. This point was subsequently corroborated by a large amount of outcrops, seismic and well information (Browne and Slatt, 2002; Mutti and Normark, 1987; Stow and Johansson, 2000). Gervais *et al.* (2006) noted that the composite pattern of lobe complex varied due to the variations in the confined degree of sedimentary topography, with confined lobe complex displaying lateral-migration stack while unconfined lobe complex displaying compensational stack. However, researches on the differential distribution of various stacking patterns, as well as their relationships with the scale of lobe complex remain to be explored.

In contrast to the lobe complex, studies of individual lobes were mostly based on outcrop observations constrained by the general low resolution of substrate seismic data. A large amount of outcrop studies showed that an individual lobe generally consisted of multiple tabular sandstones bounded by parallel or subparallel surfaces (Mutti and Normark, 1991), displaying a general coarsening and thickening-upward sequence (Macdonald *et al.*, 2011) though variations may exist at proximal, middle and distal part (Sullivan et al., 2000). Recently, however, researchers questioned the traditional notion that thickening-upward sequence was the identification mark of individual lobes, and proposed that an individual lobe, same as lobe complex, was also composed of smaller architecture unites by compensational stack (Deptuck *et al.*, 2008; Prélat *et al.*, 2010; Prélat and Hodgson, 2013). Therefore, two contrasting views, steady aggradation—progradation or compensational stack, stand on the stacking pattern of individual lobes.

Compared with the study of composite pattern and sedimentary features, researches on the quantitative scale of submarine lobes are relatively rare. Barnes and Normark (1985) first noted that the width of modern submarine lobes ranged from 1—2 km to hundreds of kilometers with thickness of 3—15 m, which, however, did not note the hierarchy of scale. By fine architecture dissection, Saller *et al.* (2008) further proved that the thickness of individual lobes averaged at 30 m while the thickness of lobe stories averaged at 10 m or so. Furthermore, Prélat *et al.* (2010) integrated the quantitative scale of submarine lobes from 6 significant submarine lobe systems around the world, noting that differences exist in the quantitative scale of confined and unconfined lobes, which might be attributed to the differences in the source nature of different systems though. So, it is necessary to conduct a further research on the differential scale under different sedimentary settings with the same source nature.

The study area of this paper lies in the deep-water zone to the south of Niger Delta Basin (Fig. 1). Lin *et al.* (2014a) studied the development pattern of submarine lobes in the shallow interval of study area (Fig. 2B) using high resolution seismic data despite the lack of well calibration. The deep interval of study area (Middle—Upper Miocene Agbada Formation, see Fig. 2B), however, bears abundant core, wireline and seismic data, and develop both basin floor and slope fan setting (Fig. 3A and B), which provides us the opportunity to investigate the detailed differences of lobe architecture between basin floor and slope fan setting. By combining multiple information, this paper conducted fine architecture characterization on both basin floor and slope fan lobe complex, with aims to (1) establish the composite patterns of lobe complex and their differential distribution under different

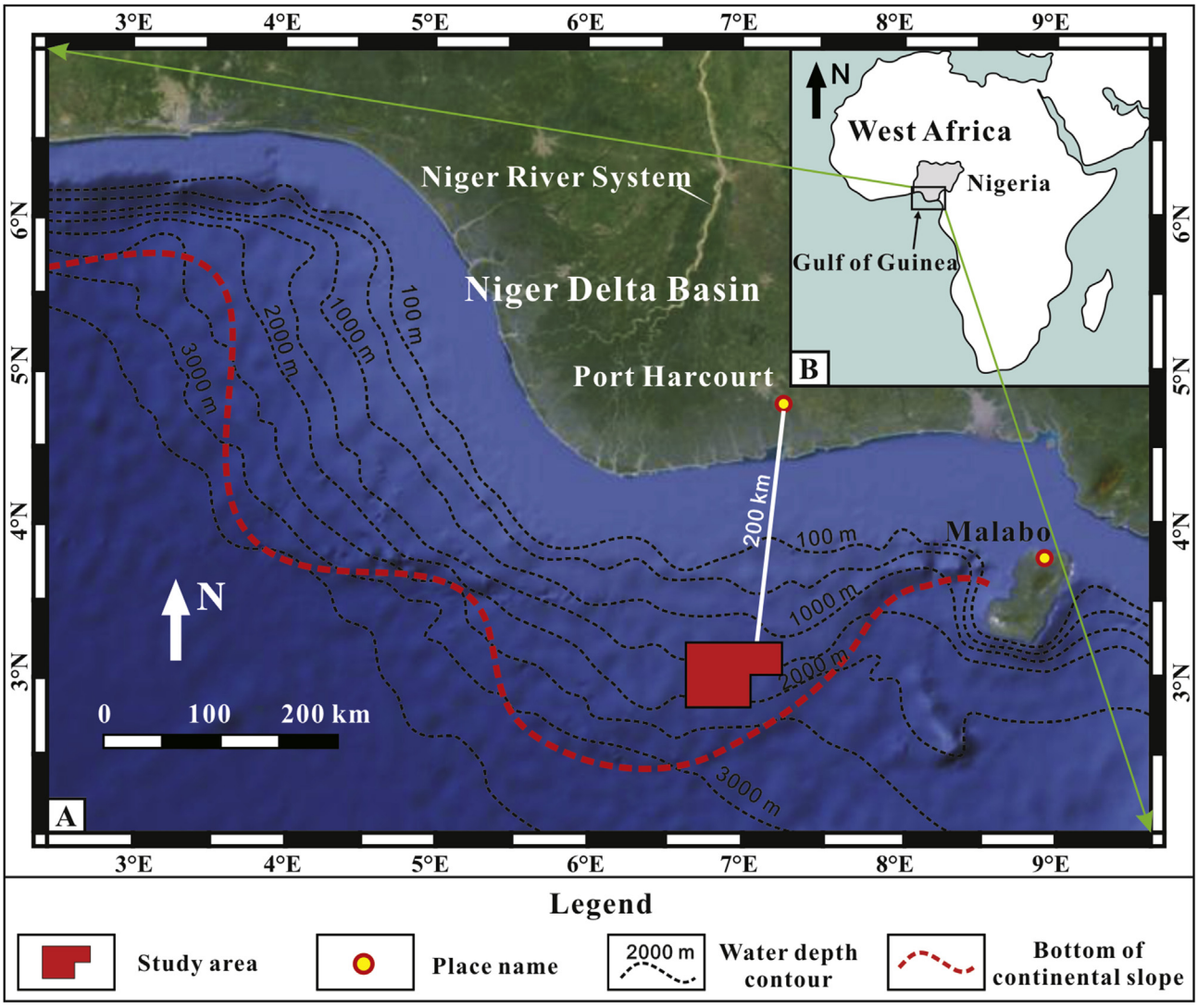

Fig. 1 Geographic map showing the location of study area at the lower continental slope of Niger Delta Basin (A) in the Gulf of Guinea, offshore West Africa (B).

sedimentary settings; (2) explore the differential scale relationships under different sedimentary settings and their controlling factors; (3) determine the stacking pattern within individual lobes and build the evolution model of individual lobes.

2. Geological setting

Our study area, covering an area of 1500 km^2 approximately, is situated in the south deep-water zone of Niger Delta Basin, with a distance of about 20 km to the north Port Harcourt. The present water depth lies between 1400 m and 1700 m, belonging to a lower continental slope setting (Fig. 1). Tectonically, the study area lies in the translational zone (intra thrust-fault belts) between the north stretch zone (tensional-fault belts) and the south crushed zone (outer thrust-fault belts) of Niger Delta Basin (Corredor *et al.*, 2005; Deng *et al.*, 2008), developing large scale thrust-related folds (Bilotti and Shaw, 2005; Briggs *et al.*, 2006; Morgan, 2003; Fig. 2B).

The Niger Delta Basin developed continuous formations from the Cretaceous to the Quaternary upwards, and involved three diachronous lithological formations (Akata Formation, Agbada Formation and Benin Formation, respectively) since the Eocene (Corredor *et al.*, 2005; Lonergan *et al.*, 2013). The target interval of this research is the Agbada Formation of the Middle—Late Miocene age (Fig. 2), developing a thick submarine deposition in the deep-water zone (Maloney *et al.*, 2010). The deep interval in the

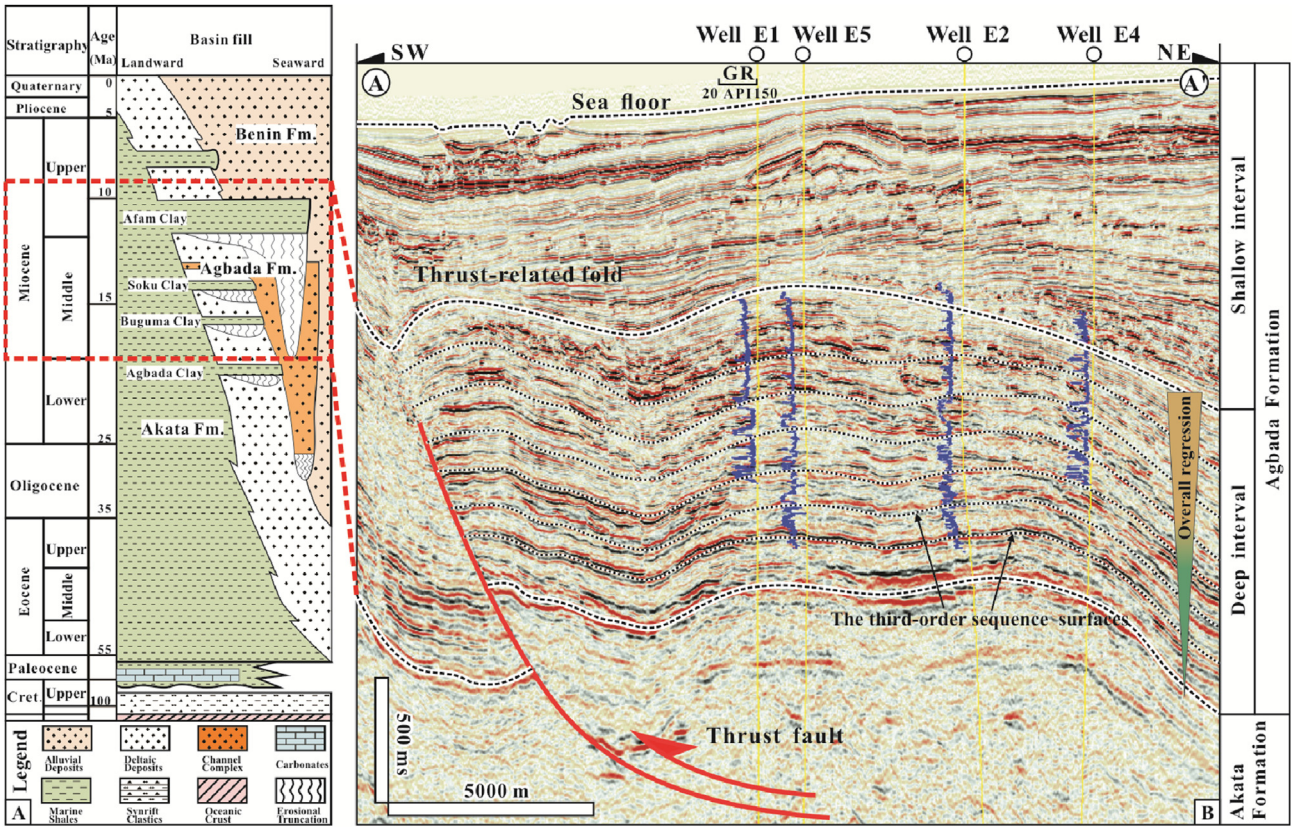

Fig. 2 Regional stratigraphic map of the Niger Delta Basin (A) (after Corredor *et al.*, 2005) and seismic section (B) showing formations and structure in the study area (see A—A′ in Fig. 3 for the position). The overall sea-level fall since the Eocene caused a trend of seaward basin filling. The deep interval in the study area contains multiple third order sequences under an overall regression setting, which develops large scale submarine-fan depositions.

study areas contains multiple 3rd-order sequences, where the lower and upper sequences exhibit much different sedimentary features: (1) The lower sequence featured as continuous high-amplitude zones with planar distribution area reaching thousands of square kilometers (Fig. 3B), which represented large scale lobe depositions. And the channelized effects were relatively weak. (2) The upper sequence, however, featured as obvious banding high-amplitude zones (Fig. 3A), representing submarine channel depositions. And relatively small scale, continuous high-amplitude zones were visible at the end of submarine channels (Fig. 3A), which represented lobe depositions with relatively strong channelized effects.

The recovered palaeotopography results from Zhao *et al.* (2012) revealed that the lower interval belonged to the deep-marine plain environment with a relatively flat, gentle, and open topography far from the source area (basin floor fan setting), while the upper interval belonged to the continental environment with a wavy, steep, and narrow topography relatively close to the source area (slope fan setting). Previous researches showed that the Niger Delta Basin had begun to enter into a large scale regression stage since the Eocene (Avbovbo, 1978; Short and Staeuble, 1967), which led to the sedimentary setting of the study area evolving from basin floor fan setting to slope fan setting progressively. This study focused on the sedimentary architecture of a slope fan lobe complex (see close-up in Fig. 3A) and a basin floor fan lobe complex (see close-up in Fig. 3B).

3. Data and methods

In this study, we focus on two hydrocarbon reservoirs of submarine lobe deposition in the deep interval. And abundant core, well logging and seismic data were collected as follows from Research Institute of China National Offshore Oil Corporation.

There are 16 wells penetrating the basin floor fan lobe reservoir with well spacing about 200 m, and 5 wells penetrating the slope fan lobe reservoir with well spacing about 1000 m (for the sake of secrecy, only a part of the wells were labeled in the plane view as shown in Fig. 3). And abundant wire logs were collected involving

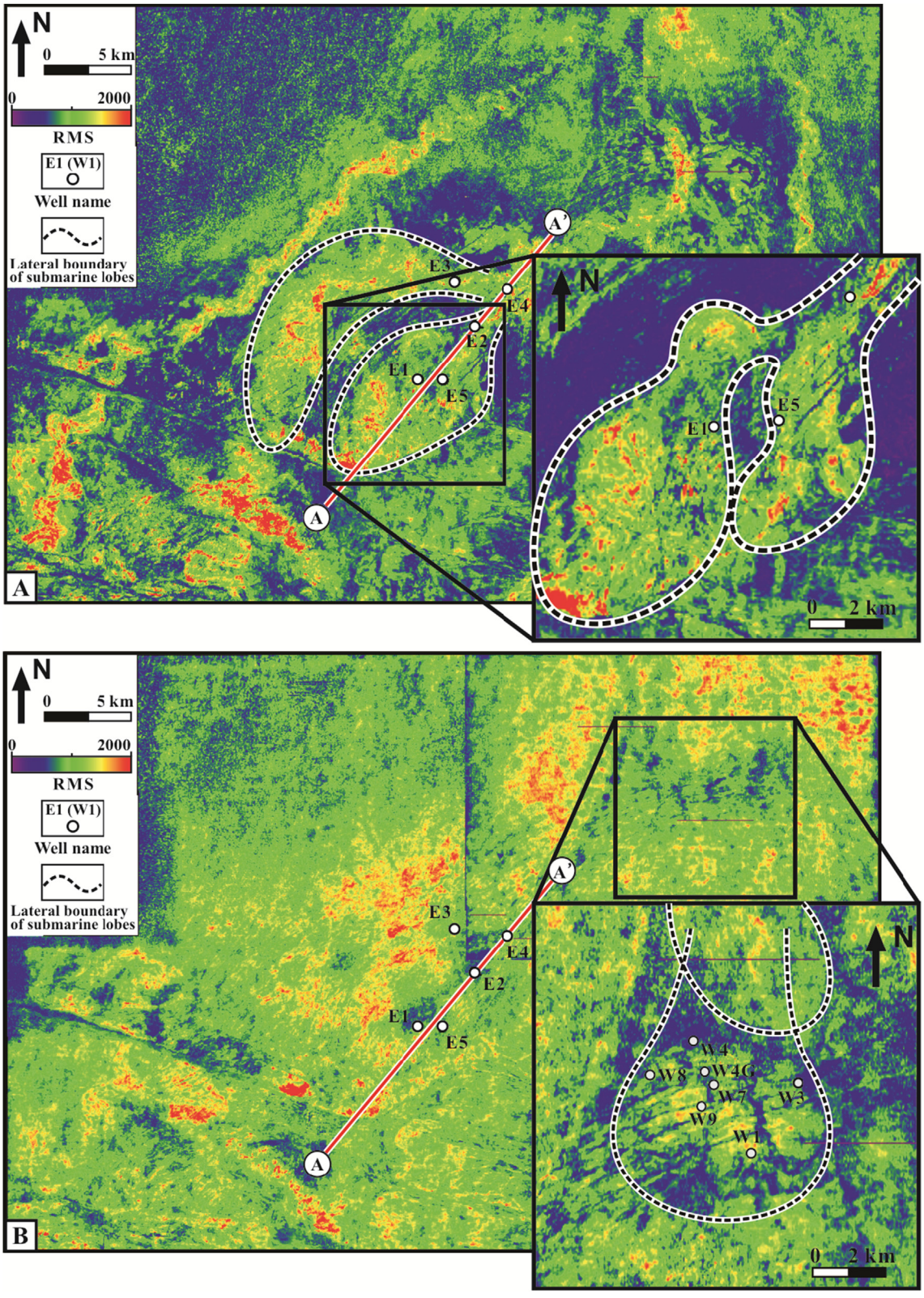

Fig. 3 RMS maps for the upper slope fan sequence with a close-up of slope fan lobe complex (A) and the lower basin floor sequence with a close-up of basin floor fan lobe complex (B). RMS maps for the whole area were extracted between two adjacent third order sequence surfaces with a time thickness of about 200—300 ms (see Fig. 2B), and the close-ups of RMS maps were extracted within a smaller time window of 40 ms above the basal third sequence surface (see Figs. 7A and 10).

gamma (GR), density (Den), acoustic time (AC), neutron porosity (NP), resistivity (RT) and so on. Two wells (Well E1, Well W4G) were systematically cored on lobe reservoirs with a cumulative length of almost 100 m and a core recovery over 90%. The two cored wells have been dealt with core location.

Seismic data were acquired on the whole study area with an inline and cross-line spacing of 12.5 m. The target interval has a dominant frequency of 32 Hz approximately, equivalent of vertical resolution of 20 m or so, based on strata velocity of 1800 m/s. The post-stack time-migrated 3D seismic data were zero phase migrated and displayed with a normal polarity, so that an increase in acoustic impedance is characterized by a red (trough)—black (peak)—red reflection combination in the seismic sections shown in this article. Sensitivity analysis of seismic attributes showed that the RMS (root mean square) seismic amplitude was the most sensitive attribute reflecting the sandbody thickness or net gross ratio. Higher RMS amplitude generally represents thicker sandbodies or larger net gross ratio within the tuning range.

The lithofacies types and features in the study area were first examined using systematic core observation and description (lithology, texture, sedimentary structure, *etc.*) on abundant cores and cuttings. And wireline logs were further combined to analyze the sedimentary sequence and well-logging response. Under the premise of well-seismic calibration, seismic attributes, seismic facies and cross sections of multiple wells were combined to recognize the lateral margin and determine the stack relationships of individual lobes. On this basis, the quantitative scale of individual lobes was measured and calculated. Based on the architecture characterization results, the differences between composite pattern and quantitative scale and the controlling factors under basin floor and slope fan settings were discussed in detail. Combined with previous researches on outcrops, architecture dissection within individual lobes was further performed by cross sections of multiple wells to discuss the stacking pattern and establish the evolution model of individual lobes.

4. Results

4.1. Lithofacies and sedimentary sequence: core and wireline responses

Based on outcrops, modern seafloor drilling and subsurface reservoir cores, the lithofacies types and features of submarine fan have been largely documented in literature, which generally agreed that the submarine fan developed various lithofacies types with complicated genetic mechanisms (Bouma, 1962; Lowe, 1982; Shanmugam, 1996, 1997). Lin *et al.* (2013, 2014b) classified 13 lithofacies from submarine channels in the study area based on researches of lithology, texture and sedimentary structure. Zhang *et al.* (2015) further elaborated on the sedimentary features of different lithofacies from submarine channels in the study area, and attributed them to five genetic mechanisms, *i.e.*, slide/slumps, debris flows, high-density turbidity currents, low-density turbidity currents, hemipelagic deposits, respectively.

Systematic core observation and description show that submarine lobes shared almost the same lithofacies types with submarine channels. The main differences, however, lie in the ratio of different lithofacies. Firstly, thick-layered massive sandstones were much more developed in submarine lobes (Fig. 4A1, A2). Such lithofacies were basically structureless with medium-coarse or fine-medium sands, corresponding to Ta division in Bouma sequence (Bouma, 1962). Their origins are still controversial presently, which were interpreted to originate from high density turbidity currents (HDTC) according to Lowe (1982), while Shanmugam *et al.* (Shanmugam *et al.*, 1985; Shanmugam and Moiola, 1991; Shanmugam, 1996, 1997, 2000, 2002, 2016) questioned the existence of high density turbidity currents due to the lack of validation of empirical data, and thus suggested an origin of sandy debris flow. Besides, the marker fluid-escape structure can always be seen (Fig. 4A3), which was generally formed by the rapid escape of pore water due to the transient overpressure during sedimentation, representing a more rapid deposition rate. In addition, parallel bedding or cross bedding fine-medium sandstones were also visible locally in submarine lobes (Fig. 4A4). Such lithofacies were generally fine-grained with good sorting, and might be connected to the modification by deep-marine tidal currents according to Shanmugam (2003, 2008, 2013). The ratio of this lithofacies, however, was much less than that of submarine channels, indicating generally weak channelized effects in submarine lobes. Moreover, submarine lobes developed smaller ratio of slump-debris flow lithofacies, which featured as abundant mud clasts floating in sandy or muddy matrix (Fig. 4A5, A6), than submarine channels, indicative of relatively steady deposition for submarine lobes.

A particular sedimentary sequence was formed by multiple lithofacies of various origins. The lobe bottom locally developed massive mud clast sand-conglomerate of slump-debris flow origin, exhibiting serrated shape of middle—low amplitude in GR curve

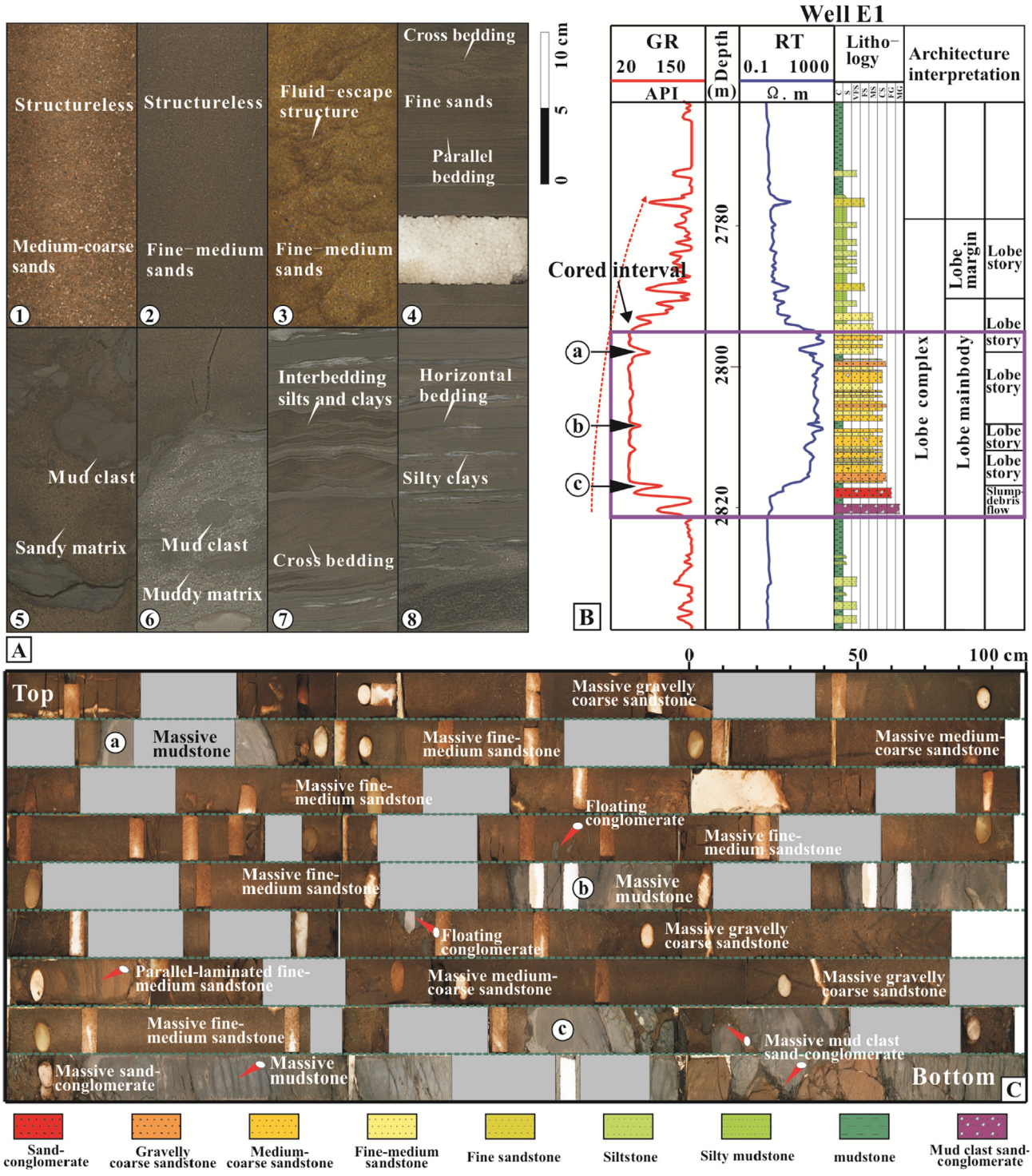

Fig. 4 Core and wireline responses showing lithofacies types and sedimentary structures (A), well-log sequence (B) and the correspondent core sequence (C) (see Fig. 3A for the well position).

(Fig. 4Bc). The lobe mainbody mainly developed fine-medium, medium-coarse, and gravelly coarse sandstones of massive structure. Also, fine sandstones with parallel bedding and floating conglomerates within massive sandstones were locally visible. All these features corresponded to a box shape of high amplitude in GR curve with slight returning, indicative of interlayers of mudstones in cores (Fig. 4Ba,Bb). In contrast, the lobe margin displayed serrated shape of low amplitude and high frequency in GR curve,

representing thin interbeddings of fine sandstone, siltstone and mudstone.

Although thickening—coarsening-upward sequence has always been regarded as the marker to recognize individual lobes (Macdonald *et al.*, 2011), the sedimentary sequences were not always the same due to the different sedimentation at different parts of lobes. For instance, a thinning—fining-upward sequence can be found at the proximal part of lobes as a result of relatively strong channelization (Fig. 5A). The middle part of lobes generally exhibited homogeneous sequences with local thin-muddy interlayers (Figs. 4 and 5B). At the distal part of lobes, however, the thickness of sandbodies decreased in couple with the increased thickness and frequency of mudstones, displaying an alternating sequence of sandstone and mudstone (Fig. 5C).

4.2. Recognition of lateral margin of individual lobes

A lobe complex is composed of multiple individual lobes, and determination of the lateral margins and stack relationships among them is the key to architecture dissection of a lobe complex, which requires an integration of seismic attributes, seismic facies, and cross sections of multiple wells.

4.2.1. Seismic attributes

The thickness of sandbodies would always thin at the composite boundary of individual lobes, which therefore would be reflected on the seismic attributes representative of sandbody thickness. As stated before, RMS amplitude was the most sensitive seismic attribute reflecting sandbody thickness or net gross ratio in study area. When the sandbody thickness varied greatly at the composite boundary of individual lobes, a distinct strip of weak amplitude within the continuous high-amplitude zone would be formed along the source direction (Fig. 6). In contrast, when the variation in sandbody thickness was not obvious at the composite boundary, the corresponding amplitude difference was not that clear in spite of recognizable traces to some degree (Fig. 7). Amplitude differences can only help to recognize the planar distribution of individual lobes, but not to determine the stack relationships among individual lobes, which should further integrate seismic sections or cross sections of multiple wells.

4.2.2. Seismic facies

Previous researches showed that lobes generally exhibited the morphology of flat bottom and convex top, the architecture of bidirectional downlap, and the structure of high continuity and high amplitude in seismic section (Gervais *et al.*, 2006; Prather *et al.*, 1998; Weimer *et al.*, 1998). Lin *et al.* (2014a, 2014b) used the wave differences on high-resolution seismic sections in the shallow interval of the study area to determine the composite boundaries and stack relationships of lobes. The deep target interval of the study area, however, had relatively low seismic dominant frequency (32 Hz), causing individual lobes to display "red—black—red" combination of high continuity and high amplitude in seismic section. At the composite boundary of individual lobes, the amplitude of seismic events weakened obviously representative of decreased sandbody thickness (Fig. 7), which corresponded to the weak-amplitude strip in the plane view (Fig. 6). Due to the lower seismic resolution, determining stack relationships between individual lobes would be difficult only based on seismic responses, which also requires the combination of well analyses.

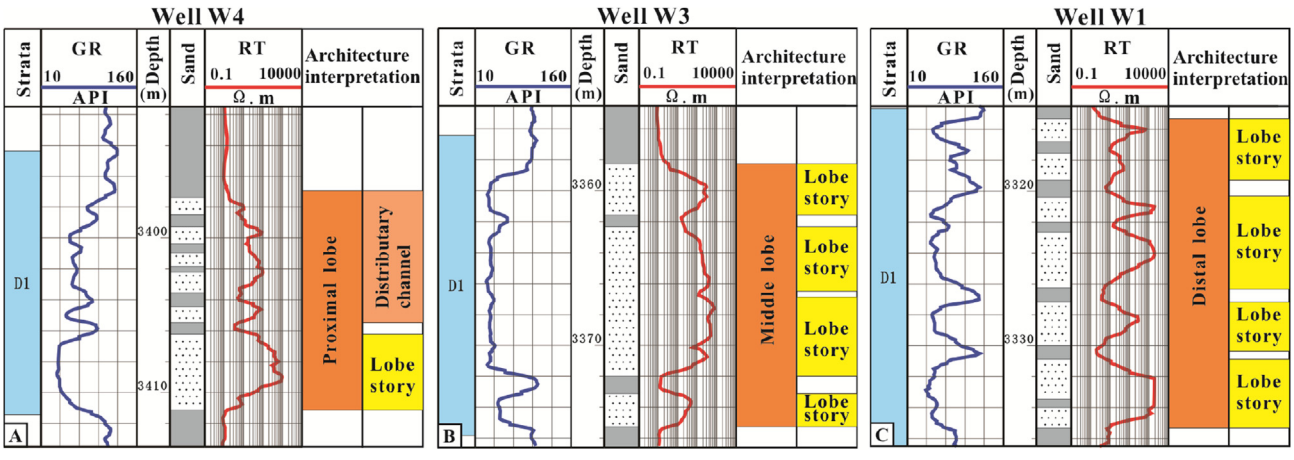

Fig. 5 Various wireline sequences of individual lobes showing a thinning—fining-upward sequence (A), a homogeneous sequence (B), and an alternating sequence of sandstone and mudstone (C) (see Fig. 3B for the well position).

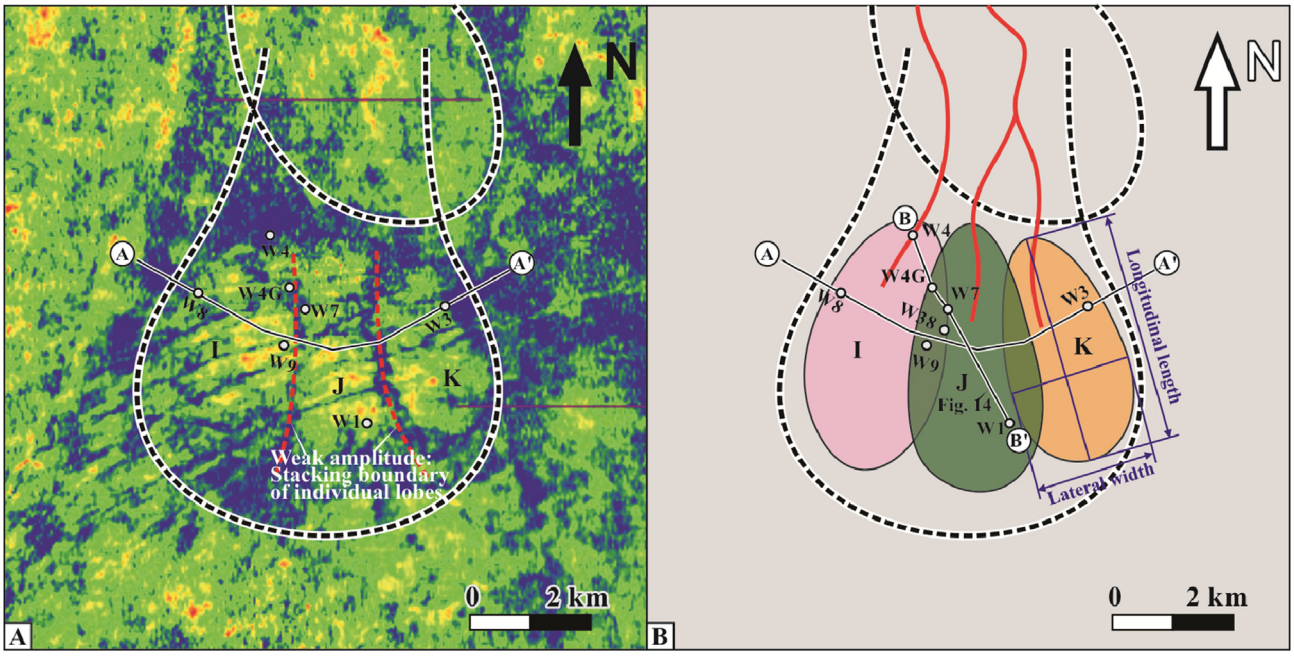

Fig. 6 RMS map of the basin floor fan lobe complex (extracted within a time window of 40 ms above the bottom surface of the lobe complex, see Fig. 7A) showing weak amplitude strip representative of the stacking boundary of individual lobes (A), and planar architecture dissection of basin floor fan lobe complex representing inordered compensational stacking patterns (B).

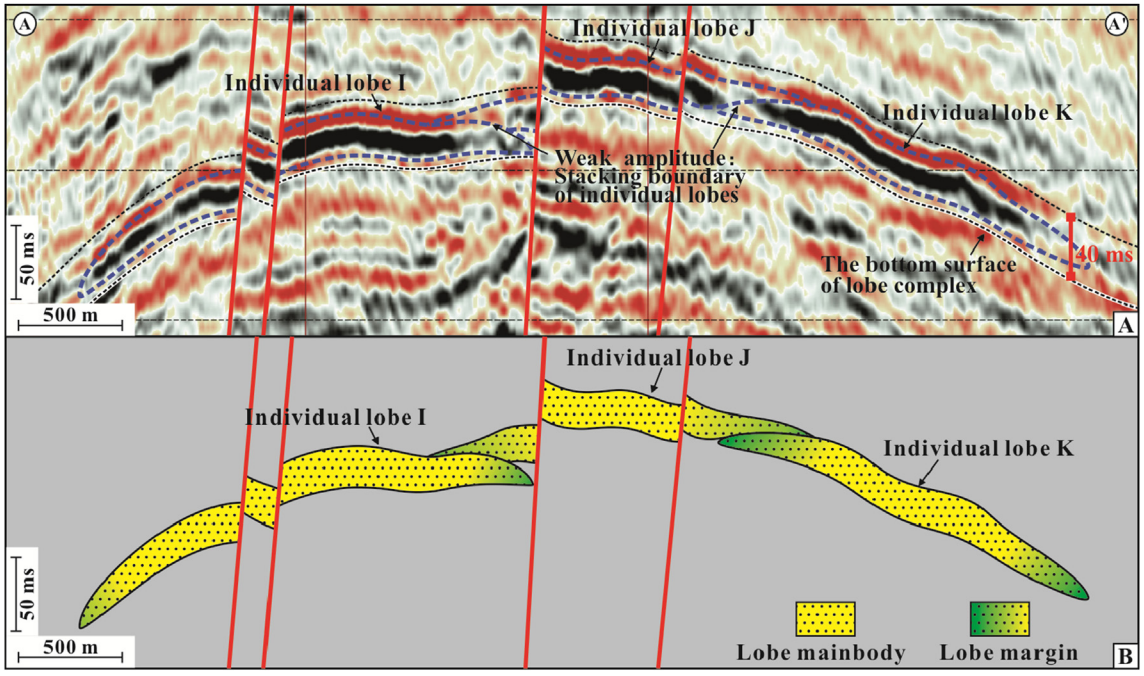

Fig. 7 Seismic section showing weak amplitude at the stacking boundary of individual lobes (A) and the architecture interpretation (B) of basin floor lobe fan complex (see A—A′ in Fig. 6 for the position).

4.2.3. Cross section of multiple wells

According to abundant practices in the dense well area, markers such as elevation differences, mudstones, and curve shape differences between wells, were always used to determine the stack relationships between sandbodies when the cross section was flattened on isochronous surface (Li *et al.*, 2012; Wen *et al.*, 2011; Yue *et al.*, 2007; Zhao *et al.*, 2013). Based on the recognition of composite boundary using

seismic information, the cross section was firstly flattened on the marked mudstones at the bottom of lobes.

When the stacked part of sandbodies was drilled by wells, such as the Well W9 and Well W38 in Fig. 8, it could be determined that the middle lobe was underlain by the west lobe with the curve shape differences and the lateral thinning trend of sandbodies thickness. However, when no well drilled the stack part of sandbodies, such as the part between Well W38 and Well W3 in Fig. 8, it could be deduced that the middle lobe was also underlain by the east lobe by the lobes' top elevation differences.

4.3. Architectural features of the target submarine lobes

By recognition of sedimentary features in single well and lateral margin between wells, architecture characterization on the basin floor fan lobe complex (Figs. 6—8) and slope fan lobe complex (Figs. 9 and 10) was performed to determine the morphology, scale and composite pattern of the lobe complex.

4.3.1. Lobe architecture of basin floor fan

The basin floor fan lobe complex exhibited fan shape in the plane view, with lateral width about 8 km and longitudinal length about 6 km (Fig. 6A). Statistics from multiple wells proved that the vertical thickness of the basin floor fan lobe complex could reach to a maximum of 30 m (averaging 20 m). The distribution of weak amplitude strip in the RMS map and the amplitude decrease in seismic sections revealed that the basin floor fan lobe complex was composed of three individual lobes (I—K), with each of them displaying an elliptical shape in the plane view (Figs. 6 and 7). Also, cross section revealed that the middle lobe (J) was underlain by the bilateral lobes (I and K), displaying unordered compensational stack in the lateral direction (Fig. 8).

Besides, differences existed in the composite degree among the individual lobes. Lobe I and lobe J were stacked by lobe margin—lobe mainbody, resulting in a relatively small decrease in the sandbody thickness (>20 m) at the composite boundary. Therefore, the wave differences in seismic section could differentiate the stack relationship between lobe I and lobe J (Fig. 7), while the weak amplitude strip in the RMS map was relatively not much clear (Fig. 6A). In contrast, lobe J and lobe K were stacked by lobe margin—lobe margin with an obvious decrease in the sandbody thickness (<20 m) at the composite boundary, which explained for the clear weak-amplitude strip between lobe J and lobe K in the RMS map (Fig. 6A) but poor resolution to differentiate the stack relationship in seismic sections (Fig. 7).

4.3.2. Lobe architecture of slope fan

The slope fan lobe complex displayed tongue shape in the plane view with lateral width about 5 km and longitudinal length about 8—10 km (Fig. 3). Statistics from single wells and time—depth conversion showed that the vertical thickness of the slope lobe complex reached to a maximum of 35 m (averaging 25 m). Integration of seismic attribute responses and 3D tracing in seismic sections revealed that the left and right slope fan lobe complex were composed of 5 (A—E) and 3 individual lobes (F—H) respectively, with planar shape varying from the oblong to the suborbicular (Fig. 9B). And the composite patterns among individual lobes exhibited both the lateral-migration stacking pattern (Fig. 10A) and the prograding stacking pattern (Fig. 10B).

Compared with the basin floor fan lobe complex, the slope fan lobe complex exhibited bigger thickness and more stacks by lobe margin—lobe mainbody with a

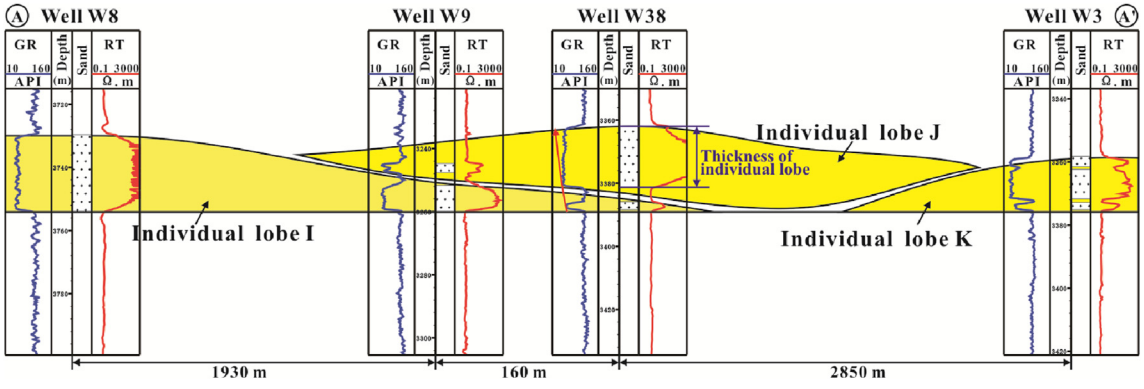

Fig. 8 Architecture features of the basin floor lobe complex indicated by the cross-well sections (see A—A′ in Fig. 6 for the position).

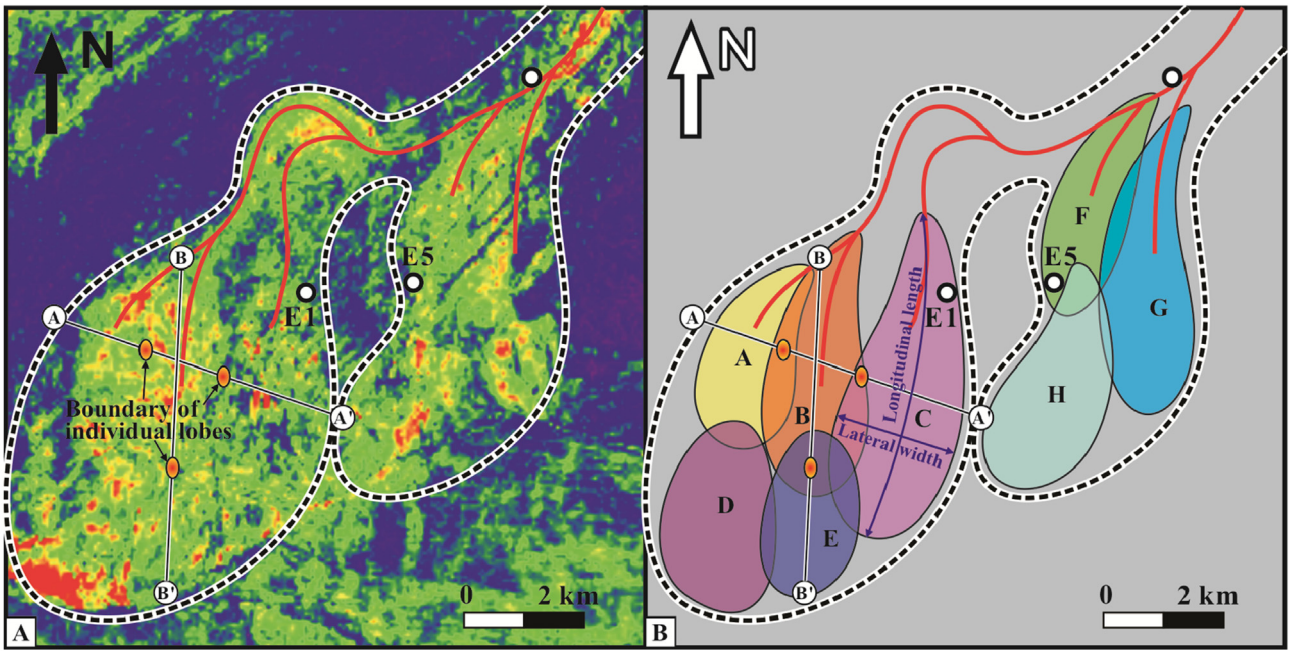

Fig. 9 RMS map of the slope fan lobe complex (extracted within a time window of 40 ms above the bottom surface of a lobe complex, see Fig. 10) showing two lobe complexes with a tongue shape (A); and the planar architecture features showing 5 individual lobes within the left lobe complex and 3 individual lobes within the right lobe complex (B).

relatively unobvious decrease in sandbody thickness at the composite boundary, which resulted in a relatively unobvious weak-amplitude response in the RMS map that could only help to recognize the composite boundary to some degree (Fig. 9A), but a clear bifurcated stacking of seismic events in seismic section (Fig. 10). In addition, due to a shallower burial depth than the basin floor fan lobe complex, the slope fan lobe complex exhibited a higher resolution in seismic section, by which echelon-stacked sandbodies (Fig. 10A) could be recognized vaguely within the individual lobes resulting from a lateral confined palaeotopography.

5. Discussions

5.1. *Differential composite patterns of lobe complex*

Architecture characterization results in the study area proved that a lobe complex was composed of multiple individual lobes by the way of compensational stack in both lateral and longitudinal direction, which corresponded to the previous points (Browne and Slatt, 2002; Mutti and Sonnino, 1981). However, differences existed in the stack relationships among individual lobes, displaying four types of compensational stacking pattern (Fig. 11): (1) Unordered type of compensational stack, featured as unordered stack relationships among individual lobes in the lateral direction; (2) Lateral migration type of compensational stack, featured as ordered, lateral migration stack relationships among individual lobes in the lateral direction; (3) Retrograding compensational stack, featured as gradually retrograding stack relationships among individual lobes in the longitudinal direction; (4) Prograding compensational stack, featured as gradually prograding stack relationships among individual lobes in the longitudinal direction.

The traditional compensational stacking pattern of lobe complex generally referred to the unordered type of compensational stack here, was generally developed in a relatively open setting (Mutti and Normark, 1987; Mutti and Sonnino, 1981). Gervais *et al.* (2006) firstly noted the lateral migration stack among individual lobes in a setting with confined topography, which we think, however, was an ordered compensational stacking pattern in essence influenced by both palaeotopography and sedimentation, thus is called lateral migration type of compensational stack here. Additionally, although Prélat and Hodgson (2013) firstly proposed the prograding and retrograding type of compensational stack, he attributed them to the compensational stacking pattern within rather than among individual lobes. However, our studies revealed that the prograding and retrograding type of compensational stack mainly developed among

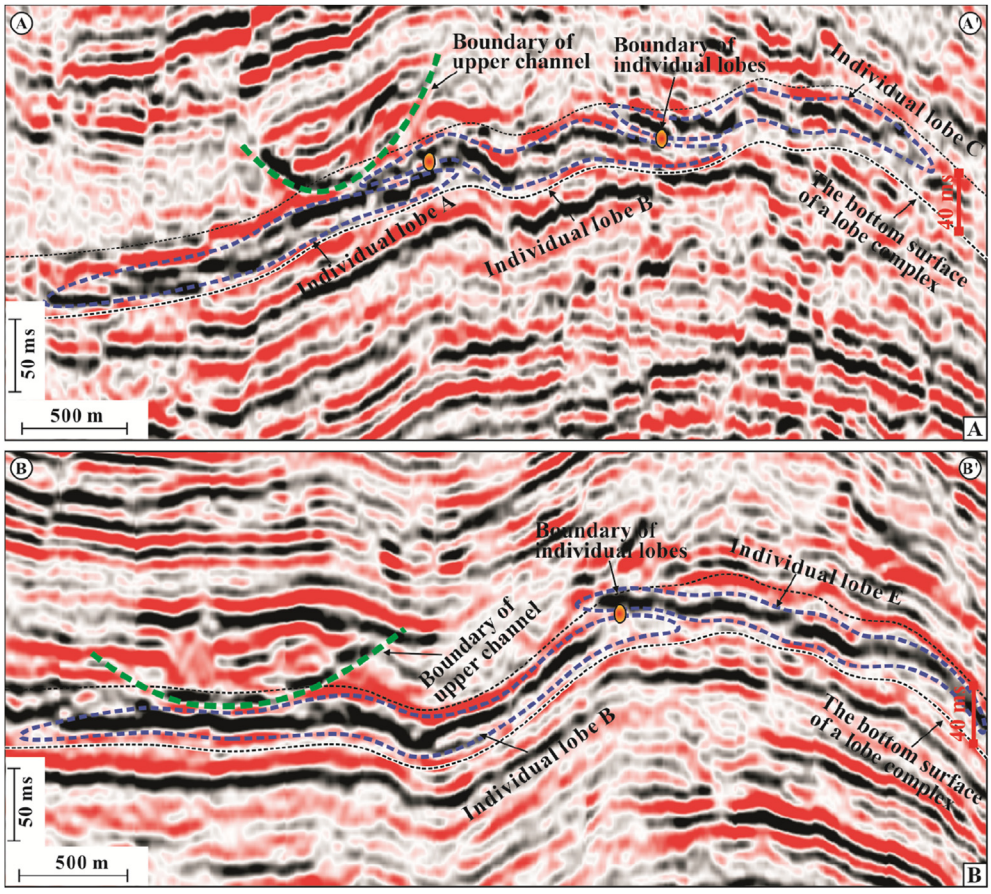

Fig. 10 Cross seismic section of the slope fan lobe complex showing lateral migration of 3 individual lobes (A) (see A—A′ in Fig. 9 for the position), and longitudinal seismic section of the slope fan lobe complex showing progradation of 2 individual lobes (B) (see B—B′ in Fig. 9 for the position).

individual lobes. And it was of high probability that the various sedimentary sequences proposed by Prélat and Hodgson (2013) was caused by compensational stack among rather than within individual lobes. It might display an upward thinning—fining sequence as the lobe mainbody was overlain by the lobe margin (*e.g.*, Well W1 in Fig. 4), while an upward thickening-coarsening sequence as the lobe mainbody was underlain by the lobe margin (*e.g.*, Well W38 in Fig. 8).

The compensational stacking pattern exhibited differential distribution under different sedimentary settings. The basin floor fan lobe complex mainly displayed the unordered type of compensational stack (Figs. 6—8), while the slope fan lobe complex mainly displayed the later three types of compensational stack (Figs. 9 and 10). The basin floor setting had a relatively open topography at the end of submarine channels with a generally weak lateral-confined degree (Laursen and Normark, 2003; Posamentier, 2003; Posamentier and Kolla, 2003; Sinclair and Cowie, 2003). Under this setting, the stacking of individual lobes was solely controlled by the sedimentation itself. As the avulsion of the supply channel happens, the next lobe has its priority to deposit at the local topographic lows caused by previous deposits, which results in a relatively stochastic stack relationship among individual lobes displaying the unordered type of compensational stack (Fig. 12A). Owing to the larger lateral accommodation space under a basin floor setting, individual lobes stack mutually by lobe margin—lobe margin in general, which makes the correspondent lobe complex display a smaller thickness, a larger lateral width, and a fan shape in the plane view (Fig. 6).

In contrast, the slope fan setting always had a narrow topography at the end of submarine channels, with a relatively strong lateral-confined degree and generally asymmetric seafloor (Beaubouef *et al.*, 1998; Burgreen and Graham, 2014; Johnson *et al.*, 2001; Prather, 2003). In this case, individual lobe prefers to deposit at the topographic lows close to the steep and more confined side. As the deposition of previous lobes continues, the next topographic lows, the position of the next individual lobe, would migrate gradually to

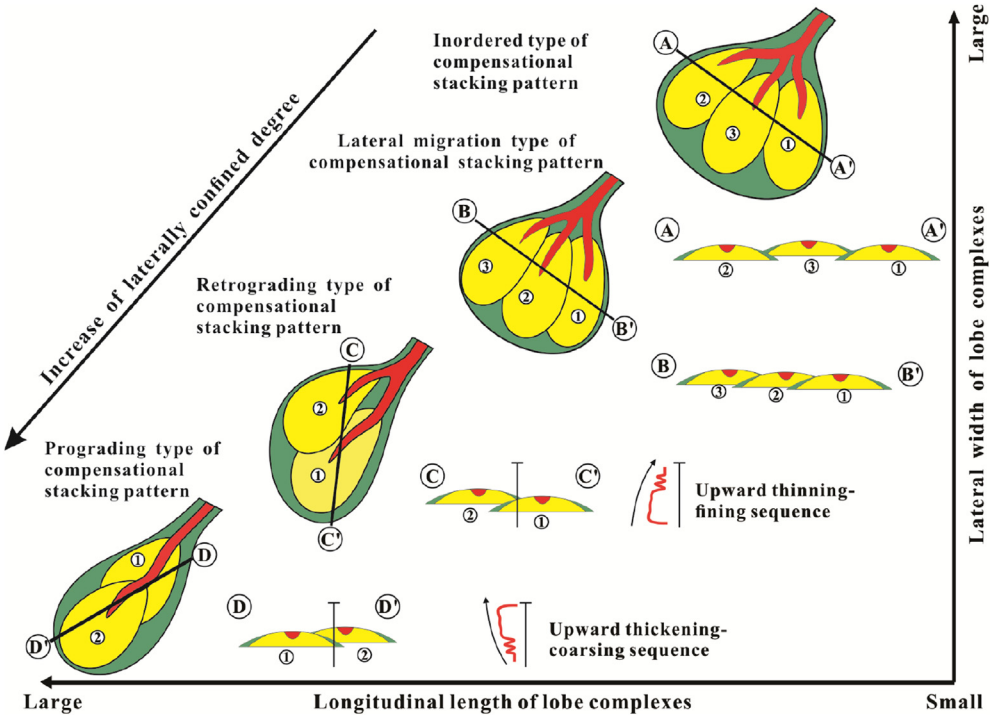

Fig. 11 Model graph illustrating inordered, lateral migration, retrograding and prograding types of the compensational stacking pattern of lobe complexes. The number represents the formation order of each individual lobe with the smaller number indicative of the earlier deposition of an individual lobe (same meanings as in Fig. 12).

the gentle and less confined side, displaying a lateral migration type of compensational stack in general (Fig. 12B). As the lateral accommodation space decreases gradually, it becomes difficult for the next individual lobe to deposit in the lateral direction. When the energy of supply channel is relatively weak, the avulsion always happens in the upstream with the new lobe depositing at the rear of previous lobes, forming the retrograding type of compensational stack. When the energy of supply channel is relatively strong, however, the supply channel tends to prograde forward cutting previous lobes, and deposits the new lobe at the front of previous lobes, forming the prograding type of compensational stack (Fig. 11). As the lateral accommodation space is limited for slope fan setting, individual lobes always stack with each other by lobe margin—lobe mainbody, making the correspondent lobe complex to display a larger thickness, a smaller lateral width but a larger longitudinal length, and a tongue shape in the plane view (Fig. 9).

As a whole, the different types of compensational stacking patterns have a great relation with the lateral

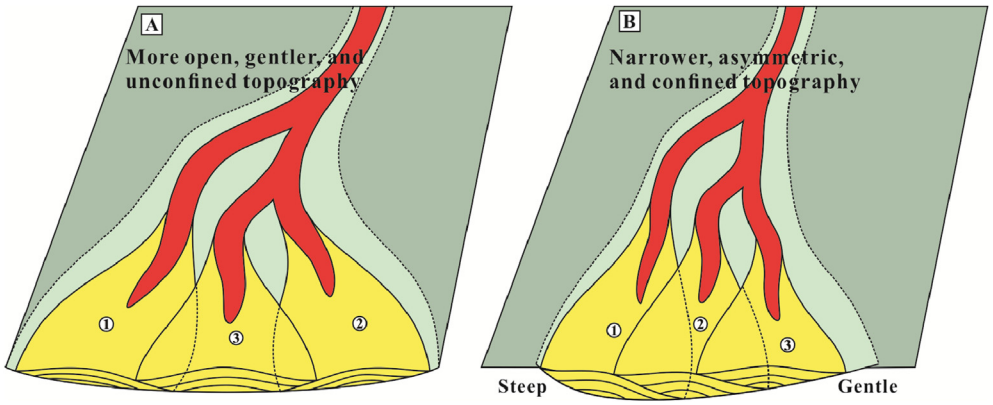

Fig. 12 Model graphs illustrating the inordered type of compensational stacking pattern of the basin floor fan lobe complex controlled by an open, gentle, and unconfined topography (A); and the lateral migration type of compensational stacking pattern of the slope fan lobe complex controlled by a narrow, asymmetric, and confined topography (B).

confined degree of palaeotopography. As the lateral confined degree of palaeotopography increases, the compensational stacking patterns evolve from the unordered type to the lateral migration type, the retrograding type and the prograding type successively, with the correspondent lobe complex exhibiting a decreased lateral width but an increased longitudinal length, and a planar evolution from fan-shape to tongue-shape gradually (Fig. 11).

5.2. Differential quantitative scale of individual lobes

To explore the quantitative scale of individual lobes, we measured the longitudinal length and lateral width of each individual lobe, and calculated the vertical thickness of each individual by statistics of single well and time—depth conversion. On this basis, the planar distribution area and volume for each individual lobe were further calculated and collected for statistics (for the various quantitative parameters, see Table 1).

As the data shown in Table 1, the individual lobe had the longitudinal length of 2—4 km, the lateral width of 1—3 km, the vertical thickness of 15—30 m, the planar distribution area of 2—9 km^2, and the volume of 65×10^6—150×10^6 m^3. Compared with this results, the lobe thickness (3—15 m) noted by Barnes and Normark (1985) was relatively smaller, which might represent the thickness of smaller lobe within individual lobes. Moreover, their minimum value of the lateral width of lobes (1—2 km) was close to that of an individual lobe in this research, while their maximum value (thousands of kilometers) might correspond to that of multiple lobe complex sets from different sources. Additionally, in comparison with the thickness of individual lobes (30 m or so) noted by Saller *et al.* (2008), this study got a smaller range, which was mainly caused by the smaller thickness of basin floor fan individual lobes (15—17 m).

Further comparison showed that obvious differences existed in the vertical thickness, the planar distribution area, and the lateral width between basin floor and slope fan individual lobes (Table 1): (1) Slope fan individual lobes exhibited larger vertical thickness (25—30 m) than that of basin floor fan individual lobes (15—20 m). (2) Slope fan individual lobes exhibited smaller planar distribution area (2.5—5.5 km^2) than that of basin floor fan individual lobes (5.5—9.0 km^2). (3) Slope fan individual lobes exhibited smaller lateral width (1—2 km) than that of basin floor fan individual lobes (2—3 km). In one word, in comparison with basin floor fan individual lobes, slope fan individual lobes displayed larger thickness, but smaller planar distribution area and lateral width, which were clearly shown on the cross plots (Fig. 13).

By integration of the quantitative scale of submarine lobes from six significant submarine lobe systems around the world, Prélat *et al.* (2010) noted that the confined individual lobes showed generally larger thickness but smaller planar distribution area relative to the unconfined individual lobes, which, however, did not exclude the influences of source nature variations for different systems. To some degree, the basin floor and slope fan individual lobes in this study were similar to the unconfined and confined individual lobes from Prélat *et al.* (2010) respectively. However, the source nature was nearly same for the basin floor and slope fan lobes in the study area, the scale differences in this work were thus mainly caused by the topographic variations for different sedimentary settings. As for the basin floor setting that has a gentle

Table 1 A summary of quantitative scale of individual lobes showing the range of various parameters and the difference between slope fan and basin floor fan individual lobes.

Sedimentary settings	Name of individual lobes	Longitudinal length (km)	Lateral width (km)	Vertical thickness (m)	Planar distribuion area (km^2)	Volume ($\times 10^6$ m^3)
Slope fan	A	2.2	1.3	25	2.7	67.5
	B	2.7	1.2	27	2.5	67.5
	C	3.0	1.5	28	5.0	140.0
	D	2.9	1.8	28	4.9	137.2
	E	2.0	1.4	27	2.8	75.6
	F	2.7	1.0	27	2.9	78.3
	G	3.9	1.3	25	4.3	107.5
	H	2.3	1.8	25	5.5	137.5
Basin floor fan	I	3.3	2.7	17	8.7	147.9
	J	3.8	2.3	15	6.0	90.0
	K	3.3	2.3	16	5.7	91.2

Note: The longitudinal length and lateral width of each individual lobe were measured on the planar architecture interpretation maps (see Figs. 6B and 9B), with errors of ±0.2 km approximately. And the vertical thickness of individual lobes was calculated by statistics of single wells (see Fig. 8) and time—depth conversion, with errors of ±2 m approximately.

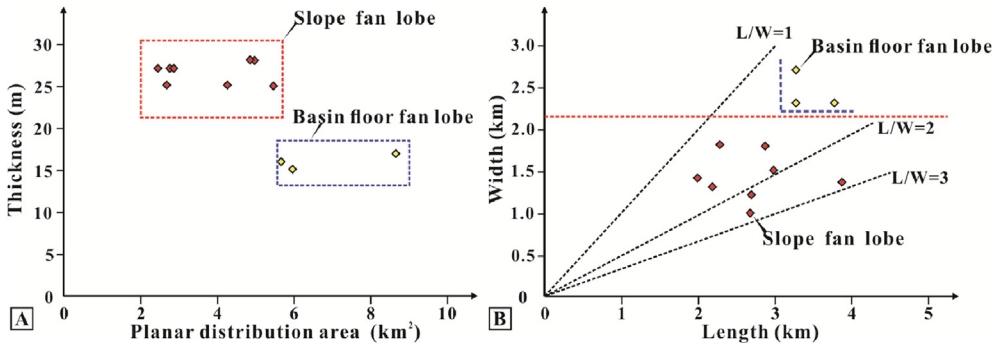

Fig. 13 Cross spots of planar distribution area *versus* thickness showing the larger thickness with smaller planar distribution area of slope fan individual lobes which is relative to that of basin floor fan individual lobes (A), and longitudinal length *versus* cross width showing a larger width of basin floor fan individual lobes relative to that of slope fan individual lobes (B).

and open topography, the vertical accommodation space is relatively small causing a limited vertical aggradation, while the lateral accommodation space is relatively large, making it easy for lobes to spread laterally; in this case, the individual lobes generally display a small thickness but extensive planar distribution. In contrast, under the slope fan setting that has a steep and narrow topography, the vertical aggradation is obviously resulted from a relatively large vertical accommodation space. However, lobes are not easy to spread laterally owing to a relatively small lateral accommodation space. As a result, the individual lobes generally exhibit a relatively large thickness but limited planar distribution.

Despite distinct differences in the vertical thickness and planar distribution area between the basin floor and the slope fan individual lobes, the differences in the volume between the both were not obvious. This phenomenon coincided with the viewpoints of Prélat *et al.* (2010), who believed that the volume of individual lobes was controlled in essence by some intrinsic factor, regardless of other extrinsic factors such as source nature, structure setting, transport distance, *etc*. We think this intrinsic factor may represent some rheological conditions when the deposition of individual lobes reached a balance. As the balance is breached, the flow state of gravity flow is not steady any more, making it easy to avulse and deposit a new individual lobe at another topographic low.

5.3. Stacking pattern and evolution model of individual lobes

As to the stacking pattern within individual lobes, two contrasting views have been documented in literature currently. One common view said that the compensational stacking pattern emerged mostly among larger scale architecture unites (larger than individual lobes in common sense), but was rarely visible in smaller scale architecture unites (Mutti and Normark, 1987; Mutti and Sonnino, 1981; Stow and Johansson, 2000; Straub *et al.*, 2009). This view had been proved by abundant outcrops (*e.g.*, deep-water lobe outcrops in the Ross Formation of Clare Basin in West Ireland and the Skoorsteenberg Formation of Tanqua Basin in South Africa) with a general point that an individual lobe was amalgamated by multiple tabular sandbodies (Sullivan *et al.*, 2000), displaying an overall upward thickening—coarsening sequence (Anderton, 1995; Lien *et al.*, 2003; Macdonald *et al.*, 2011; Pyles, 2008). These features were in great difference with those of the compensational stacking pattern.

Another contrasting view, however, suggested that the compensational stacking pattern was ubiquitous regardless of the scale of architecture unites (Deptuck *et al.*, 2008; Prélat and Hodgson, 2013; Prélat *et al.*, 2010; Schlager, 2004, 2010). Prélat and Hodgson (2013) pointed that an individual lobe was compensationally stacked by multiple lobe stories displaying various vertical sequences. However, as was discussed before, it was highly possible that the various vertical sequences were formed by the compensational stack among rather than within individual lobes. Moreover, Straub *et al.* (Straub and Pyles, 2012; Straub *et al.*, 2009) questioned the scale-invariant view by theoretical calculation, and affirmed definitely that an individual lobe was composed of multiple tabular sandbodies by the way of steady aggradation or progradation. And Lin *et al.* (2014b) got the same conclusion by examination in detail on the outcrop of deep-water lobes in Gannan area of China, which had a similar sedimentary setting to the study area in this paper. This paper, by architecture dissection within individual lobes in dense-well zone, further

substantiated that the multiple lobe stories constructed an individual lobe by the steady aggradation or progradation, rather than by the compensational stack with each other.

As the architecture dissection within individual lobes (Fig. 14) showed, different parts of an individual lobe manifested different sedimentary combination features. (1) The proximal lobe (Well W4) developed bell-shaped branch channels locally on the top, which cut the underlain funnel-shaped tabular sandbodies. (2) The middle lobe (Well W7) developed thick box-shaped sandbodies (about 16 m) with rare muddy interlayers. (3) The distal lobe (Well W1) developed a combination of multiple thin funnel-shaped sandbodies (3—4 m for a single sandbody) with muddy interlayers frequently developed. (4) The lobe margin (the upper part in Well W1, the lower part in Well W7) developed alternating fine sandstones, siltstones and mudstones with a finger shape in GR curves.

As a whole, transversely from the lobe mainbody to the lobe margin, the thickness of lobe stories within individual lobes decreased gradually in couple with a decrease in the amalgamated degree and fining of lithology. Longitudinally from proximal lobe to distal lobe, the top branch channels disappeared gradually, and the amalgamated degree of lobe stories decreased as well, with muddy interlayers developed gradually. This variation trend of architecture generally coincided with the outcrop observation of Gannan area in China. However, abundant massive transport deposits (MTDs), which featured as a large amount of mud clasts, were also found at the bottom of proximal lobe in outcrops, and disappeared gradually towards the middle—distal lobe (Lin *et al.*, 2014b). This kind of MTDs was generally believed to originate from slump-debris flow deposits at the early stage of submarine lobes (Garziglia *et al.*, 2008; Sawyer *et al.*, 2007). Although the MTDs were not further interpreted on the cross sections of multiple wells due to an obscure feature in well logs, the coring of lobe sequence was described before substantiated their existence.

To sum up, an individual lobe generally comprises three smaller architecture unites, *i.e.*, bottom MTDs, middle tabular sandbodies, and top branch channels, respectively. The middle tabular sandbodies are formed by the way of steady aggradation—progradation pattern. The differential architecture combinations suggested a three-stage evolution model of individual lobes according to the gravity flow types and the gradually evolved energy.

1) Rapid accumulation of debris flow (Fig. 15A). At the initial stage of deposition of individual lobes, the topographic slope decreases abruptly with the terrain turning into open as well. In this case, the velocity of gravity flow decreases abruptly, thus sediments of various particle sizes carried by the gravity flow accumulated rapidly, forming slump-debris flow deposits (MTDs). This stage featured as abundant mud clasts as a result of the strong erosion on the underlain muddy strata.
2) Progradation of turbidity flow (Fig. 15B). As the deposition of MTDs continues, on one hand, the gravity flow is diluted and evolves into turbidity flow gradually; on the other hand, the slope gradient decreases as well, causing a weakened

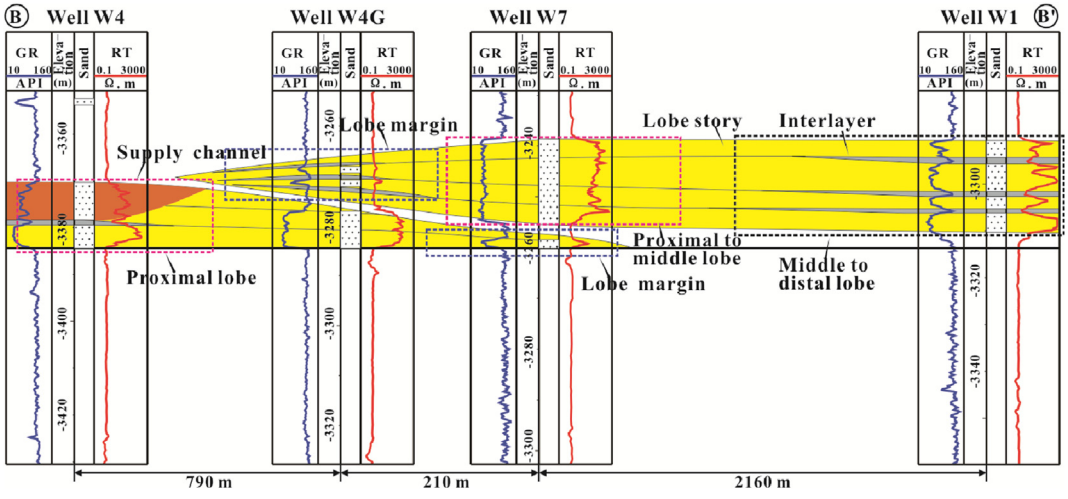

Fig. 14 Architecture features within individual lobes indicated by cross-well section showing both transverse and longitudinal variations of the facies association, thickness and amalgamation degree of lobe stories (GR = Gamma; RT = Resistivity; see Fig. 6B for the B—B′ position).

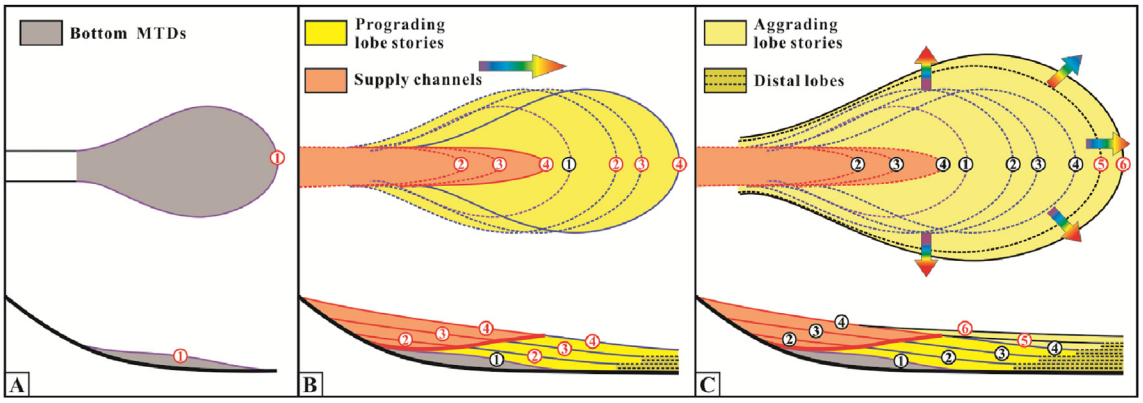

Fig. 15 Mode patterns illustrating the three evolution stages of an individual lobe with the rapid accumulation of debris flow (A), the progradation of turbidity flow (B), and the aggradation of turbidity flow (C). The number represents the formation order of lobe stories as well as the corresponding progradation of supply channels. The number with red color represents the deposition of current stage, while the number with black color represents the deposition of former stage.

variation in the velocity of turbidity flow which has a steady flow state. During this stage, the top branch channels prograde forward and deposit sediments gradually because of a strong capability of transport and erosion, which forms the constantly prograding tabular sandbodies.

3) Aggradation of turbidity flow (Fig. 15C). With the thickness of individual lobes increasing gradually, the gravity flow is further diluted in couple with a further decreased slope gradient. At this stage, the top branch channels stop prograding any more due to a weak capability of transport and erosion, and fine-grained sediments begin to overflow and aggrade, forming aggrading tabular sandbodies. As the aggradation continues, the deposition of individual lobes reaches a balance gradually; in this case, top branch channels and upstream supply channels are blocked up, and avulse locally to deposit the next individual lobe with the previous lobe entering into the abandoned stage.

As a whole, from the initiation to the abandonment of an individual lobe, the gravity flow is diluted gradually in couple with the gradually decreased erosion energy, and the sedimentary process goes through three evolution stages as "rapid accumulation—progradation—aggradation". During the whole evolution process of an individual lobe, the gravity flow types evolve gradually with a relatively steady flow state. When the individual lobe reaches a balance, the flow state of gravity flow will abruptly change in couple with the avulsion of supply channels. In this case, compensationally stacked with previous individual lobes, a new individual lobe begins to form a larger scale lobe complex.

6. Conclusions

Based on analyses of architecture features of the basin floor and slope lobe complexes in the deep interval of the study area, the following conclusions were achieved.

1) A lobe complex is composed of multiple individual lobes by the way of compensational stacking pattern. Based on the stacking relationships among individual lobes, four types of compensational stacking pattern are classified as the inordered type, the lateral migration type, the retrograding type and the prograding type. Under the basin floor setting which has a relatively open topography with a generally weak laterally confined degree, the lobe complex is dominated by the inordered type of compensational stacking pattern, exhibiting fan shape in the plane view, with relatively large lateral width but relatively small thickness. In contrast, under the slope setting which has a narrow topography with a relatively strong laterally confined degree, the lobe complex is dominated by lateral migration, retrograding and prograding types of compensational stacking pattern, showing a tongue shape in the plane view, with relatively small lateral width but relatively large thickness.
2) Individual lobes show an oblong to suborbicular shape in the plane view, and have the lateral width of 1—3 km, the longitudinal length of 2—4 km, the aspect ratio of 1—3, the planar distribution area of 2.5—9 km^2, and the vertical thickness of 15—30 m. The basin floor setting has a smaller vertical but

larger lateral accommodation space, which causes correspondingly more extensive planar distribution of individual lobes with smaller thickness. In contrast, the slope setting has a larger vertical but smaller lateral accommodation space, and correspondingly the individual lobes are characterized by more limited planar distribution but larger thickness.

3) An individual lobe is composed of multiple tabular sandbodies by the way of steady aggradation or progradation, which is greatly different from the compensational stacking pattern of lobe complexes. An individual lobe generally comprises three smaller architecture units, *i.e.*, bottom MTDs (massive transport deposits), middle tabular sandbodies, and top branch channels, respectively. From proximal lobe to middle and distal lobe, the bottom MTDs and top branch channels disappear gradually, and the amalgamated degree of middle tabular sandbodies decreases as well, with muddy interlayers developed gradually. With the evolution of gravity flow types, the formation of an individual lobe generally includes three stages as "rapid accumulation—progradation—aggradation".

Acknowledgements

This study is supported by the National Planned Major Science and Technology Projects of China (No. 2011ZX05030-005-02). We thank the China National Offshore Oil Corporation for providing the subsurface data and permitting publication. We thank our colleagues, Wen-Jie Feng, Zhen Li, Mei Huang, Ya-Fei Jing and Qin-Yu Xia for their help on the seismic data interpretation and analysis. We also would like to appreciate the Editor-in-Chief of *JoP*, Prof. Zeng-Zhao Feng, Prof. G. Shanmugam and one anonymous reviewer for their insightful reviews and constructive suggestions to make the paper a better contribution.

References

Anderton, R., 1995. Sequences, cycles and other nonsense: are submarine fan models any use in reservoir geology? In: Hartley, A.J., Prosser, D.J. (Eds.), *Characterization of Deep Marine Clastic Systems, Geological Society, London, Special Publications, 94*, pp. 5—11.

Avbovbo, A.A., 1978. Tertiary lithostratigraphy of Niger delta. *AAPG Bulletin*, 62(2), 295—300.

Barnes, N.E., Normark, W.R., 1985. Diagnostic parameters for comparing modern submarine fans and ancient turbidite systems. In: Bouma, A.H., Normark, W.R., Barnes, N.E. (Eds.), *Submarine Fans and Related Turbidite Systems*. Springer-Verlag, New York, pp. 13—14.

Beaubouef, R.T., Abreu, V., Van Wagoner, J.C., 2003. Basin 4 of the Brazos—Trinity slope system, western Gulf of Mexico: the terminal portion of a late Pleistocene lowstand systems tract. In: *GCSSEPM Proceedings*, pp. 45—66.

Beaubouef, R.T., Garfield, T.R., Goulding, F.J., 1998. Seismic stratigraphy of depositional sequences: high resolution images from a passive margin slope setting, offshore West Africa. *AAPG Bulletin*, 82, 1890.

Bilotti, F., Shaw, J.H., 2005. Deep-water Niger Delta fold and thrust belt modeled as a critical-taper wedge: the influence of elevated basal fluid pressure on structural styles. *AAPG Bulletin*, 89(11), 1475—1491.

Bouma, A.H., 1962. *Sedimentology of Some Flysch Deposits: A Graphic Approach to Facies Interpretation*. Elsevier, p. 168.

Briggs, S.E., Davies, R.J., Cartwright, J.A., Morgan, R., 2006. Multiple detachment levels and their control on fold styles in the compressional domain of the deepwater west Niger Delta. *Basin Research*, 18(4), 435—450.

Browne, G.H., Slatt, R.M., 2002. Outcrop and behind-outcrop characterization of a Late Miocene slope fan system, Mt. Messenger Formation, New Zealand. *AAPG Bulletin*, 86(5), 841—862.

Burgreen, B., Graham, S., 2014. Evolution of a deep-water lobe system in the Neogene trench—slope setting of the East Coast Basin, New Zealand: lobe stratigraphy and architecture in a weakly confined basin configuration. *Marine and Petroleum Geology*, 54, 1—22.

Chapin, M.A., Davies, P., Gibson, J.L., 1994. Reservoir architecture of turbidite sheet sandstones in laterally extensive outcrops, Ross Formation, Western Ireland. In: Weimer, P., Bouma, A.H., Pettingill, H.S. (Eds.), *Gulf Coast Section Society of Economic Paleontologists and Mineralogists Foundation Fifteenth Annual Research Conference*. Society of Economic Paleontologists, Gulf Coast Section (GCSSEPM) Foundation, Houston, pp. 53—68.

Corredor, F., Shaw, J.H., Bilotti, F., 2005. Structural styles in the deep-water fold and thrust belts of the Niger Delta. *AAPG Bulletin*, 89(6), 753—780.

Deng, R.J., Deng, Y.H., Yu, S., Hou, D.J., 2008. Hydrocarbon geology and reservoir formation characteristics of Niger Delta Basin. *Petroleum Exploration and Development*, 35(6), 755—762 (in Chinese with English abstract).

Deptuck, M.E., Piper, D.J.W., Savoye, B., Gervais, A., 2008. Dimensions and architecture of late Pleistocene submarine lobes off the northern margin of East Corsica. *Sedimentology*, 55(4), 869—898.

Garziglia, S., Migeon, S., Ducassou, E., Loncke, L., Mascle, J., 2008. Mass-transport deposits on the Rosetta province (NW Nile deep-sea turbidite system, Egyptian margin): characteristics, distribution, and potential causal processes. *Marine Geology*, 250(3—4), 180—198.

Gervais, A., Savoye, B., Mulder, T., Gonthier, E., 2006. Sandy modern turbidite lobes: a new insight from high

resolution seismic data. *Marine and Petroleum Geology*, 23(4), 485—502.
Johnson, S.D., Flint, S., Hinds, D., De Ville Wickens, H., 2001. Anatomy, geometry and sequence stratigraphy of basin floor to slope turbidite systems, Tanqua Karoo, South Africa. *Sedimentology*, 48(5), 987—1023.
Laursen, J., Normark, W.R., 2003. Impact of structural and autocyclic basin-floor topography on the depositional evolution of the deep-water Valparaiso forearc basin, central Chile. *Basin Research*, 15(2), 201—226.
Li, Z.P., Lin, C.Y., Dong, B., Bu, L.X., 2012. An internal structure model of subaqueous distributary channel sands of the fluvial-dominated delta. *Acta Petrolei Sinica*, 33(1), 101—105 (in Chinese with English abstract).
Lien, T., Walker, R.G., Martinsen, O.J., 2003. Turbidites in the upper Carboniferous Ross Formation, western Ireland: Reconstruction of a channel and spillover system. *Sedimentology*, 50(1), 113—148.
Lin, Y., Wu, S.H., Wang, X., Lu, Y., Wan, Q.H., Zhang, J.J., Zhang, Y.K., 2013. Research on architecture model of deepwater turbidity channel system: a case study of a deepwater research area in Niger Delta Basin, West Africa. *Geological Review*, 59(3), 510—520 (in Chinese with English abstract).
Lin, Y., Wu, S.H., Wang, X., Wan, Q.H., Zhang, J.J., Zhang, W.B., 2014a. Reservoir quality differences of submarine fans in deep-water oilfield A in Niger Delta Basin, West Africa. *Oil and Gas Geology*, 35(4), 494—502 (in Chinese with English abstract).
Lin, Y., Wu, S.H., Wang, X., Zhao, X.M., Ling, Y., Lu, Y., Zhang, J.J., 2014b. Research on reservoir architecture models of deep-water turbidite lobes. *Natural Gas Geoscience*, 25(8), 1197—1204 (in Chinese with English abstract).
Lonergan, L., Jamin, N.H., Jackson, C.A.L., Johnson, H.D., 2013. U-shaped slope gully systems and sediment waves on the passive margin of Gabon (West Africa). *Marine Geology*, 337, 80—97.
Lowe, D.R., 1982. Sediment gravity flows: II, depositional models with special reference to the deposits of high-density turbidity currents. *Journal of Sedimentary Petrology*, 52(1), 279—297.
Macdonald, H.A., Peakall, J., Wignall, P.B., Best, J., 2011. Sedimentation in deep-sea lobe-elements: implications for the origin of thickening-upward sequences. *Journal of the Geological Society*, 168(2), 319—332.
Maloney, D., Davies, R., Imber, J., Higgins, S., King, S., 2010. New insights into deformation mechanisms in the gravitationally driven Niger Delta deep-water fold and thrust belt. *AAPG Bulletin*, 94(9), 1401—1424.
Morgan, R., 2003. Prospectivity in ultradeep water: the case for petroleum generation and migration within the outer parts of the Niger Delta apron. In: Arthur, T.J., Macgregor, D.S., Cameron, N.R. (Eds.), *Petroleum Geology of Africa: New Themes and Developing Technologies, Geological Society, London, Special Publications, 207*, pp. 151—164.
Mutti, E., Normark, W.R., 1987. *Comparing examples of modern and ancient turbidite systems: ancient turbidite systems: problems and concepts*. In: *Marine Clastic Sedimentology*. Springer, Netherlands, pp. 1—38.
Mutti, E., Normark, W.R., 1991. An integrated approach to the study of turbidite systems. In: Weimer, P., Link, M.H. (Eds.), *Seismic Facies and Sedimentary Processes of Submarine Fans and Turbidite Systems*. Springer-Verlag, New York, pp. 75—106.
Mutti, E., Sonnino, M., 1981. Compensation cycles: a diagnostic feature of turbidite sandstone lobes. In: *International Association of Sedimentologists; 2nd European Regional Meeting, Italy (Bologna). Int. Assoc. Sedimentol. Special Publication*. Oxford, p. 5.
Posamentier, H.W., 2003. Depositional elements associated with a basin floor channel-levee system: case study from the Gulf of Mexico. *Marine and Petroleum Geology*, 20(6—8), 677—690.
Posamentier, H.W., Kolla, V., 2003. Seismic geomorphology and stratigraphy of depositional elements in deep-water settings. *Journal of Sedimentary Research*, 73(3), 367—388.
Prather, B.E., 2003. Controls on reservoir distribution, architecture and stratigraphic trapping in slope settings. *Marine and Petroleum Geology*, 20(6—8), 529—545.
Prather, B.E., Booth, J.R., Steffens, G.S., Craig, P.A., 1998. Classification, lithologic calibration, and stratigraphic succession of seismic facies of intraslope basins, deep-water Gulf of Mexico. *AAPG Bulletin*, 82(5A), 701—728.
Prélat, A., Covault, J.A., Hodgson, D.M., Fildani, A., Flint, S.S., 2010. Intrinsic controls on the range of volumes, morphologies, and dimensions of submarine lobes. *Sedimentary Geology*, 232(1), 66—76.
Prélat, A., Hodgson, D.M., 2013. The full range of turbidite bed thickness patterns in submarine lobes: controls and implications. *Journal of the Geological Society*, 170(1), 209—214.
Prélat, A., Hodgson, D.M., Flint, S.S., 2009. Evolution, architecture and hierarchy of distributary deep-water deposits: a high-resolution outcrop investigation from the Permian Karoo Basin, South Africa. *Sedimentology*, 56(7), 2132—2154.
Pyles, D.R., 2008. Multiscale stratigraphic analysis of a structurally confined submarine fan: Carboniferous Ross Sandstone, Ireland. *AAPG Bulletin*, 92, 557—587.
Reading, H.G., Richards, M., 1994. Turbidite systems in deep-water basin margins classified by grain size and feeder system. *AAPG Bulletin*, 78(5), 213—235.
Saller, A., Werner, K., Sugiaman, F., Cebastiant, A., May, R., Glenn, D., 2008. Characteristics of Pleistocene deep-water fan lobes and their application to an upper Miocene reservoir model, offshore East Kalimantan, Indonesia. *AAPG Bulletin*, 92(7), 919—949.
Sawyer, D.E., Flemings, P.B., Shipp, R.C., Winker, C.D., 2007. Seismic geomorphology, lithology, and evolution of the late Pleistocene Mars—Ursa turbidite region, Mississippi Canyon area, northern Gulf of Mexico. *AAPG Bulletin*, 91(2), 215—234.
Schlager, W., 2004. Fractal nature of stratigraphic sequences. *Geology*, 32, 185—188.
Schlager, W., 2010. Ordered hierarchy versus scale invariance in sequence stratigraphy. *International Journal of Earth Sciences*, 99, S139—S151.

Shanmugam, G., 1996. High-density turbidity currents: are they sandy debris flows? *Journal of Sedimentary Research*, 66, 2—10.

Shanmugam, G., 1997. The Bouma sequence and the turbidite mind set. *Earth-Science Reviews*, 42, 201—229.

Shanmugam, G., 2000. 50 years of the turbidite paradigm (1950s—1990s): deep-water processes and facies models—a critical perspective. *Marine and Petroleum Geology*, 17(2), 285—342.

Shanmugam, G., 2002. Ten turbidite myths. *Earth-Science Reviews*, 58(3), 311—341.

Shanmugam, G., 2003. Deep-marine tidal bottom currents and their reworked sands in modern and ancient submarine canyons. *Marine and Petroleum Geology*, 20(5), 471—491.

Shanmugam, G., 2008. The constructive functions of tropical cyclones and tsunamis on deep-water sand deposition during sea level highstand: implications for petroleum exploration. *AAPG Bulletin*, 92(4), 443—471.

Shanmugam, G., 2013. Modem internal waves and internal tides along oceanic pycnoclines: challenges and implications for ancient deep-marine baroclinic sands. *AAPG Bulletin*, 97(5), 851—857.

Shanmugam, G., 2016. Submarine fans: a critical retrospective (1950—2015). *Journal of Palaeogeography*, 5(2), 110—184.

Shanmugam, G., Damuth, J.E., Moiola, R.J., 1985. Is the turbidite facies association scheme valid for interpreting ancient submarine fan environments? *Geology*, 13, 234—237.

Shanmugam, G., Moiola, R.J., 1991. Types of submarine fan lobes: models and implications. *AAPG Bulletin*, 75(75), 156—179.

Short, K.C., Staeuble, A.J., 1967. Outline of geology of Niger delta. *AAPG Bulletin*, 51, 761—779.

Sinclair, H.D., Cowie, P.A., 2003. Basin-floor topography and the scaling of turbidites. *The Journal of Geology*, 111(3), 277—299.

Stow, D.A.V., Johansson, M., 2000. Deep-water massive sands: nature, origin and hydrocarbon implications. *Marine and Petroleum Geology*, 17, 145—174.

Straub, K.M., Paola, C., Mohrig, D., Wolinsky, M.A., George, T., 2009. Compensational stacking of channelized sedimentary deposits. *Journal of Sedimentary Research*, 79, 673—688.

Straub, K.M., Pyles, D.R., 2012. Quantifying the hierarchical organization of compensation in submarine fans using surface statistics. *Journal of Sedimentary Research*, 82(11), 889—898.

Sullivan, M., Jensen, G., Goulding, F., Jennette, D., Foreman, L., Stern, D., 2000. Architectural analysis of deep-water outcrops: implications for exploration and development of the Diana Sub-basin, western Gulf of Mexico. In: *Deep-water Reservoirs of the World: Gulf Coast Section SEPM Foundation 20th Annual Research Conference*. Houston, pp. 1010—1032.

Walker, R.G., 1978. Deep-water sandstone facies and ancient submarine fans: models for exploration for stratigraphic traps. *AAPG Bulletin*, 62, 932—966.

Weimer, P., Slatt, R.M., 2006. *Introduction to the petroleum geology of deepwater settings*. In: *AAPG Studies in Geology, SEPM Special Publication*,, 57, pp. 1—10.

Weimer, P., Varnai, P., Budhijanto, F.M., Acosta, Z.M., Martinez, R.E., Navarro, A.F., Rowan, M.G., McBride, B.C., Villamil, T., Arango, C., Crews, J.R., Pulham, A.J., 1998. Sequence stratigraphy of Pliocene and Pleistocene turbidite systems, northern green Canyon and Ewing bank (offshore Louisiana), northern Gulf of Mexico. *AAPG Bulletin*, 82(5), 918—960.

Wen, L., Wu, S., Wang, Y., Yue, D., Li, Y., 2011. An accurate method for anatomizing architecture of subsurface reservoir in mouth bar of fluvial dominated delta. *Journal of Central South University (Science and Technology)*, 42(4), 1072—1078 (in Chinese).

Yue, D., Wu, S., Liu, J., 2007. An accurate method for anatomizing architecture of subsurface reservoir in point bar of meandering river. *Acta Petrolei Sinica*, 28(4), 99—103 (in Chinese).

Zhang, J., Wu, S., Wang, X., Lin, Y., Fan, H., Jiang, L., 2015. Reservoir quality variations within a sinuous deep water channel system in the Niger Delta Basin, offshore West Africa. *Marine and Petroleum Geology*, 63, 166—188.

Zhao, X., Bao, Z., Liu, Z., Zhao, H., Chai, Q., 2013. An in-depth analysis of reservoir architecture of underwater distributary channel sand bodies in a river dominated delta: a case study of T51 Block, Fuyu Oilfield. *Petroleum Exploration and Development*, 40(2), 181—187 (in Chinese).

Zhao, Y., Bao, Z., Wang, X., Sun, L., Yan, L., Chen, Z., 2012. Control factors of a submarine fan in Niger Basin. *Journal of Xi'an Shiyou University (Natural Science Edition)*, 27(2), 6—12 (in Chinese).